# *(Invited) Mechanically Flexible Integrated Photonic Systems for Sensing and Communications*

# *(Invited)* Mechanically Flexible Integrated Photonic Systems for Sensing and Communications

Lan Li[a], Hongtao Lin[a], Jerome Michon[a], Sarah Geiger[a,b], Junying Li[a], Hanyu Zheng[a], Yizhong Huang[a], Anupama Yadav[c], Kathleen Richardson[c], Tian Gu[a], and Juejun Hu[a]

[a] Department of Materials Science and Engineering, Massachusetts Institute of Technology, Cambridge, Massachusetts 02139, USA
[b] Department of Materials Science and Engineering, University of Delaware, Newark, Delaware 19716, USA
[c] College of Optics and Photonics, CREOL, Department of Materials Science and Engineering, University of Central Florida, Orlando, Florida 32816, USA

Conventional integrated photonic devices are fabricated on rigid semiconductor or dielectric substrates and are therefore inherently incompatible with soft biological tissues. Over the past few years, we have developed a suite of active and passive photonic devices and systems integrated on plastic substrates which can be bent, twisted, and stretched without compromising their optical performance. Here we review the latest progress in this emerging field, and discuss the rational material and mechanical engineering principles underlying the extraordinary flexibility of these photonic structures. Leveraging these design strategies, we demonstrated bendable glass waveguide circuits, flexible waveguide-integrated nanomembrane photodetectors, and stretchable photonics.

## Introduction

Since the first proposal of integrated photonic circuits by S. Miller in 1969 (1), integrated photonics, which involves a multitude of miniaturized optical components connected by an optical waveguide network on one single substrate, has thrived over the past decades and is now widely regarded as a transformative paradigm shift in optics and photonics analogous to integrated circuits revolutionizing the electronic industry. Whether it is the archetypal "laser beam circuitry" on a glass plate envisaged by S. Miller or state-of-the-art photonic chips diced from a silicon or InP wafer, integrated photonics platforms demonstrated thus far are pre-dominantly fabricated on rigid substrates. What if we can make flexible integrated photonic devices that can be bent, twisted, and stretched?

The success paradigm of flexible electronics, a close analogy of flexible photonics, provides a convincing answer. Flexible electronics, which dates back to the 1960s (2), is now a booming 5.13 billion US dollar market with a projected compound annual growth rate (CAGR) of 21% (3). Compared to traditional electronic components integrated on rigid substrates, their flexible counterparts are often lighter, more compact and more durable (with improved impact resistance), and are therefore witnessing rapidly increasing adoption in consumer electronic products. The mechanical compliance of flexible electronics enables conformal integration on biological tissues such as human skin for continuous health monitoring (4), as well as minimally invasive implantable medical devices with significantly reduced risk of tissue damage (5). Flexible devices are

also compatible with roll-to-roll (R2R) manufacturing, an extremely high-throughput, cost-effective solution to large-area applications such as photovoltaics and display. In the same vein, flexible photonics is starting to reap these benefits: for instance, R2R printed flexible optical waveguide sensors now claim drastically reduced cost ideal for single-use/disposable applications with production length up to hundreds of meters (6, 7).

In addition to the processing and deployment advantages already well-recognized in the flexible electronics community, adding photonics into the picture further furnishes numerous intriguing opportunities beyond the current capabilities of flexible electronics. Light is the preferred carrier for ultra-high bandwidth data communications and is inherently immune to electromagnetic interference (EMI); spectroscopic signatures extracted from optical measurements provide unambiguous information about chemical species; and there are also many applications which rely on light-matter interactions and inevitably involves photonics technologies, such as lighting, imaging, and display. As one specific application example leveraging the unique benefits of photons, flexible optical waveguides are currently being pursued for board-level data communications to replace conventional electrical interconnects in order to improve datacenter energy efficiency and bandwidth density, where their mechanical flexibility facilitates high-density, low-cost packaging and assembly (8-12). Flexible and stretchable photonic structures can also be conformally integrated on arbitrary curvilinear optical surfaces to impart unconventional functions (e.g., aberration compensation) to the optical element underneath (13, 14). Last but not least, mechanical deformation presents a simple and elegant approach for broadband photonic device tuning and reconfiguration (15-18).

Flexible photonic devices were traditionally fabricated using polymers exploiting the inherent mechanical flexibility of organic polymer materials (19-22). These all-polymer devices, however, suffer from several drawbacks. In terms of optical properties, the accessible range of refractive indices in common optical polymers is limited to 1.45-1.7 (23), posing a severe constraint on photonic designs. The presence of C-H bonds in many polymers causes parasitic optical absorption in the near-infrared due to the chemical bond's $2^{nd}$ and $3^{rd}$ order vibrational overtones (23). From a device processing perspective, few polymers can withstand high processing temperatures (> 400 °C), which limits their integration capacity with other material systems. Furthermore, the inferior optoelectronic properties of polymers largely prohibit their applications in active components. Therefore, unleashing the full potential of flexible photonics mandates further expansion of its material repertoire beyond organic polymers.

Glass, traditionally regarded as a fragile substance, is a somewhat surprising candidate in the search for next-generation materials for flexible integrated photonics. Chalcogenide glasses (ChGs), the amorphous compounds of S, Se, and/or Te, are particularly attractive for this application, since they can be monolithically deposited and processed at low temperatures (< 200 °C) on organic polymer substrates, and their high refractive indices ($n$ > 2) provide strong optical confinement, allowing tight bends with minimal radiative loss. Besides ChGs, several amorphous thin film materials (which are not classical glasses) such as $TiO_2$ and a-Si also claim some of the aforementioned advantages of ChGs and have been used in flexible photonics fabrication (24, 25). Following the approach, we have demonstrated a series of flexible photonic devices which we review in the following sections (18, 26-29).

## Multi-neutral-axis design enabled foldable photonics

Fig. 1a illustrates the generic fabrication process of passive ChG flexible photonic devices. The process starts with coating an epoxy polymer (SU8 negative resist, MicroChem Corp.) layer on a rigid handler substrate (oxide coated Si wafer), followed by evaporation deposition and lithographic patterning of ChG thin films to define the photonic devices. Substrate heating measured during ChG film deposition is negligible (< 5 °C for $Ge_{23}Sb_7S_{70}$ glass) and thus the substrate is maintained at near room temperature throughout the process. 2.5-D multi-layer structures can also be fabricated simply by repeating the epoxy-coating/deposition/patterning steps: the excellent planarization capability of SU-8 epoxy ensures high pattern fidelity during subsequent lithographic steps not affected by underlying topology from device layers underneath. The monolithic process circumvents the need to transfer devices between different substrates to significantly improve the fabrication yield and throughput and is compatible with standard semiconductor microfabrication technologies. In the last step, the photonic devices are delaminated from the handler substrate using a Kapton tape to form free-standing flexible structures.

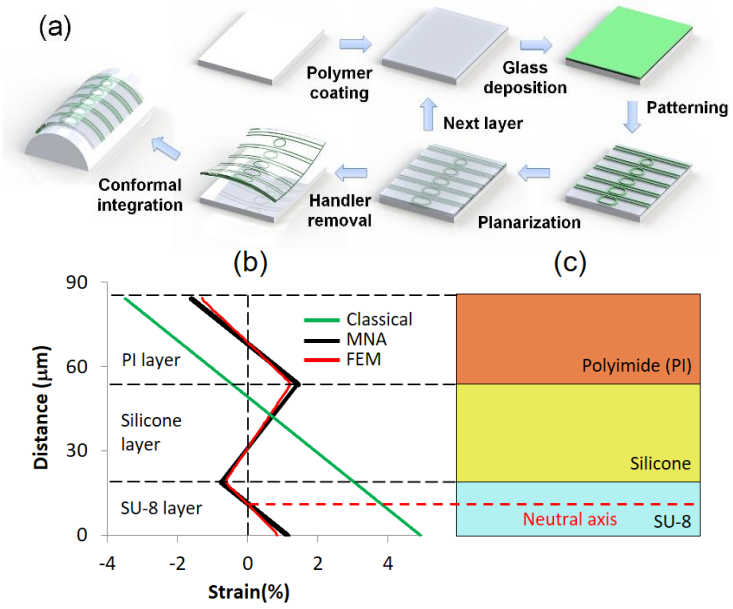


Figure 1. (a) Fabrication process sequence of passive flexible photonic devices; (b) strain distribution in the flexible structure calculated using the classical multilayer bending theory, the multi-neutral-axis (MNA) theory and finite element method (FEM) simulations; (c) schematic cross-sectional structure of the flexible photonic structure after delamination: the red dotted line indicates the location of the neutral axis in the SU-8 layer (27).

Fig. 1c illustrates the layer structure of the resulting flexible chip. Since the bi-layer Kapton tape consists of a silicone rubber adhesive film and a polyimide substrate, the delaminated flexible chip assumes an “Oreo” geometry with the soft silicone layer (Young’s modulus ~ 1 MPa) sandwiched between two stiff layers (the Young’s moduli of polyimide and SU-8 are both ~ 2 GPa). Interestingly, we have identified that the classical multilayer beam bending theory fails to provide a correct strain distribution in the structure. This is because significant shear deformation is introduced in the soft silicone layer upon bending due to the large elastic modulus mismatch between the layers, which violates the assumption that cross-sectional planes remain planar after bending

underlying the classical bending theory. We have therefore derived a new multi-neutral-axis (MNA) theory taking into account the effect and the analytical MNA framework has been validated through finite element simulations (Fig. 1b) as well as our strain-optical coupling measurements (27).

The new MNA theory specifies that a neutral axis emerges in the SU-8 layer where the strains vanish. Consequently, the structure can readily accommodate large bending deformations without damaging the devices by placing the glass devices at the neutral axis. The configuration further allows significant degrees of freedom in device engineering. Unlike the classical bending theory which stipulates a single neutral axis near the center of the entire multilayer stack, the location of the neutral axis in SU-8 can be flexibly tuned by adjusting the layer thicknesses and moduli in the laminated structure such that the optical devices can be placed at difference locations to meet specific application needs.

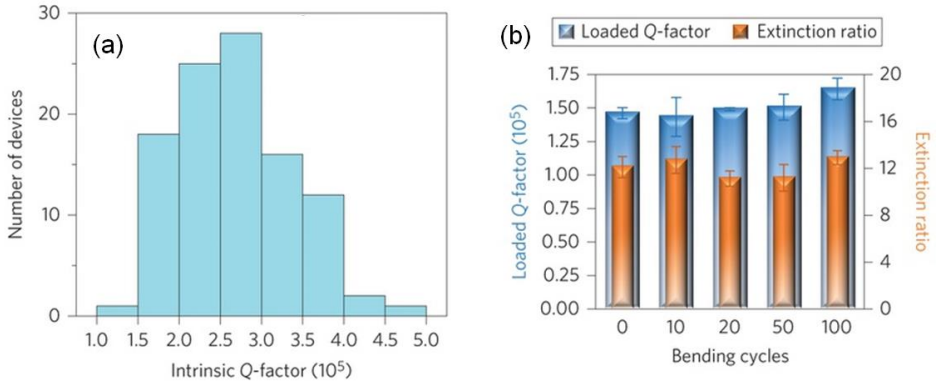


Figure 2. (a) Q-factor distribution measured in flexible micro-disk resonators; (b) Q-factors and extinction ratios of the resonator after multiple bending cycles at a bending radius of 0.5 mm (27).

Following the MNA design, we have demonstrated foldable optical devices boasting both record optical performance and extraordinary mechanical flexibility. Fig. 2a is a histogram showing the distribution of intrinsic optical quality factors (Q-factors) in flexible micro-disk resonators measured near 1550 nm wavelength. Our best device exhibited a Q-factor of $4.6 \times 10^5$, the highest value reported for photonic devices on plastic substrates. To test the mechanical reliability of the flexible devices, optical transmittance of the resonators was measured after repeated bending cycles with a bending radius of 0.5 mm. Fig. 2b shows that there were minimal variations in Q-factor and extinction ratio after multiple bending cycles. The device therefore far outperforms traditional flexible photonic components based on semiconductor NMs or those integrated on ultra-thin glass substrates which can only sustain bending radius down to several millimeters.

## Stretchable integrated photonics

A truly flexible photonic module ought to be both bendable and stretchable. The ability of a functional substrate to tolerate stretching deformation is essential for wrinkle-free conformal integration on general curvilinear surfaces (e.g. spherical surfaces), which is also mandatory for epidermal sensors, as human skin exhibits stretchability up to 20%. Using epoxy polymers as the substrate supports bending to sub-millimeter radius as we

discussed in the preceding section, however precludes stretching deformation. Instead, elastomers are the only practical substrate options for simultaneously bendable and stretchable photonics (30).

Photonic integration on elastomer substrates, however, presents a severe technical barrier. First of all, elastomers are known for their gigantic coefficient of thermal expansion (CTE). For example, polydimethylsiloxane (PDMS) has a CTE of 310 ppm, far greater than that of Si (2.6 ppm) or $Ge_{23}Sb_7S_{70}$ glass (20.8 ppm). High-quality optical thin film deposition directly on PDMS is therefore not possible due to the large CTE mismatch. The CTE mismatch also leads to resist film cracking and poor pattern fidelity. Secondly, while elastomers are highly stretchable, most optical materials cannot sustain tensile strain of more than a few percent. Last but not least, stretching results in geometric deformation of photonic components which inevitably modifies their optical responses. Such changes destabilize device operation, in particular for applications such as sensing where a stable baseline is of paramount importance.

To address these challenges, we have devised a strategy combining both material engineering and micro-mechanical design. We chose $Ge_{23}Sb_7S_{70}$ glass as our main optical material, given its good chemical and thermal stability (compared to the archetypal ChG compositions $As_2S_3$ and $As_2Se_3$ which are prone to surface oxidation (31)), low deposition temperature, as well as established low loss optical performance (32). The device fabrication process follows that in Fig. 1a. During the polymer coating step, a PDMS film and an SU-8 layer are sequentially spin coated. The PDMS layer functions as the substrate, whereas SU-8, having an intermediate CTE of 52 ppm, is sandwiched between $Ge_{23}Sb_7S_{70}$ glass and PDMS to relieve thermal stress caused by the CTE mismatch between PDMS and glass.

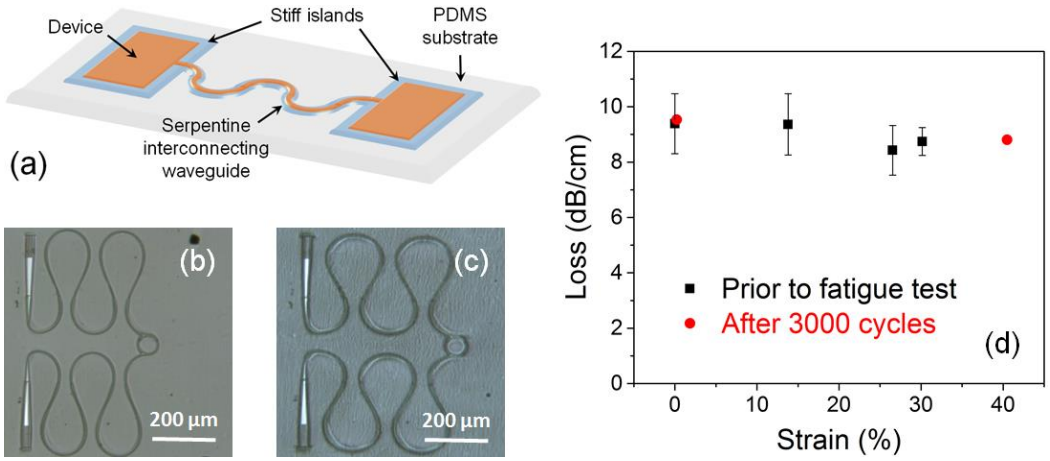


Figure 3. (a) Schematic layout of an integrated photonic chip design to enable large stretchability while minimizing undesired strain-induced wavelength shift in critical optical devices; (b) & (c) top-view micrographs of a stretchable device (b) at 0% strain and (c) the same device at 36% tensile strain; (d) measured optical loss in a micro-resonator prior to and after a mechanical fatigue test consisting of 3,000 stretching cycles at 42% tensile strain (33).

Fig. 3a schematically illustrates the design concept of a stretchable photonic circuit, which comprises isolated stiff "islands" connected by stretchable optical waveguides. The design stabilizes device operation while maintaining large stretchability. Photonic components sensitive to geometry changes are located on the rigid "islands" in the form

of lithographically patterned SU-8 pads and thereby minimizing their deformation. To transform SU-8 and $Ge_{23}Sb_7S_{70}$ glass, both brittle materials, into stretchable waveguide structures, we patterned both layers into a serpentine shape. The meandering geometry can withstand large tensile deformation without structural damage in a way similar to stretching a helix-shaped spring (34).

Fig. 3b shows a top-view optical microscope image of a prototypical stretchable device consisting of two grating couplers for input and output light coupling from optical fibers, a micro-ring resonator, and serpentine single-mode ChG waveguides connecting the components following the design in Fig. 3a. Since the operation wavelength of grating couplers critically depends on the grating period, the grating couplers are placed on SU-8 islands to prevent undesired strain-induced wavelength drift. The device is mounted on a home-built optical testing station to characterize its optical response in-situ while the device is strained. Fig. 3c shows the same device after applying a tensile strain (elongation) of 36% on the PDMS substrate clearly showing the in-plane deformation of the serpentine waveguides. Close optical microscopy inspection reveals that the device can sustain repeated stretching without cracking or damage. Fig. 3d plots the optical propagation loss in the micro-ring resonator measured at different strain states, both before and after a fatigue test consisting of 3,000 stretching cycles at 42% tensile strain. No measurable loss change was observed despite the large applied tensile strain. The result proves that mechanically robust stretchable photonic devices can be made from glass materials which are brittle in their bulk state, without degradation of optical performance. The general micro-mechanical design principles are equally applicable to other material systems, thereby enabling flexible and stretchable optical systems to be constructed out of a diverse range of materials regardless of their intrinsic mechanical behavior.

## Active-passive photonic integration on flexible substrates

In the previous sections, we focus on flexible photonic systems containing only passive elements, such as optical waveguides, gratings, and resonators. A complete photonic integrated circuit (PIC) entails active optoelectronic devices such as light sources, modulators, switches and photodetectors interconnected by a waveguide network. We have therefore taken the first step towards a flexible PIC by demonstrating a waveguide-integrated nanomembrane photodetector. Compared to conventional normal incidence photodetectors which collect optical radiation incident from free-space, waveguide-integrated detectors are not only essential building blocks for PICs but also claim a number of performance advantages such as noise suppression and high-speed response (35, 36).

The glass waveguide-integrated NM detector structure is schematically illustrated in Fig. 4a. The photodetector employs a lateral metal-semiconductor-metal (MSM) structure consisting of an InGaAs semiconductor nanomembrane optical absorber layer with a pair of gold electrodes juxtaposed on both sides of a ChG waveguide. Light propagating in the waveguide is directed to the InGaAs mesa and is absorbed by the semiconductor to create electron-hole pairs. When a voltage bias is applied across the two electrodes, the photo-generated charged carriers in InGaAs can cross the Schottky barrier between the metal electrode and the semiconductor, leading to a photocurrent which scales with the incident light intensity.

The device was fabricated following the procedures below. An SU-8 layer is first spin coated on a handler wafer. An InP die with an epitaxially grown InGaAs layer is bonded

onto the wafer with the epi-layer facing the substrate. The SU-8 film serves as an adhesive in the bonding process. The InP die is subsequently removed by mechanical lapping followed by wet chemical etching, leaving behind the InGaAs absorber NM of about 200 nm in thickness. The NM is lithographically patterned and wet etched to form the detector mesa. Glass waveguides and metal electrodes are then fabricated on top of the NM mesa to define the detector structure. In the last step, the flexible device supported by the SU-8 film is delaminated from the handler wafer. Fig. 4b presents an SEM micrograph of the completed device.

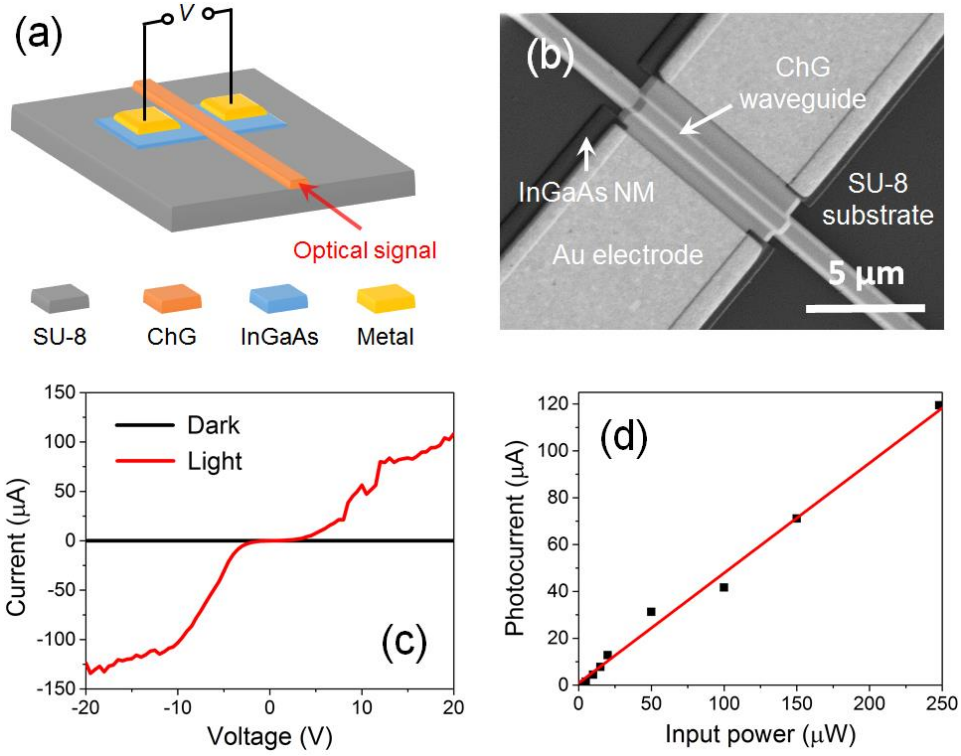


Figure 4. (a) Schematic diagram of the glass waveguide-integrated photodetector; (b) SEM micrograph of a detector; (c) I-V response of the detector in dark and under illumination; (d) photocurrent of the detector as a function of input optical power in the waveguide (33).

During testing, optical signal was launched into the waveguide from an optical fiber probe and the electrical response was monitored using a pair of micro-probes. The fabricated detector device was mounted on a motion stage during optoelectronic characterizations such that it can be mechanically buckled in-situ at varying bending radii. Fig. 4c plots the current-voltage (I-V) curves of the detector measured in dark and under illumination with 250 µW incident optical power at 1550 nm wavelength. The device shows a negligible saturation dark current of 0.5 nA at 10 V bias. The photocurrent increases linearly with increasing optical power, as shown in Fig. 4d. Slope of the response curve yields a responsivity of 0.5 A/W at 1550 nm, corresponding to an external quantum efficiency of 40%. Our bending tests shows that dark current and photo response of the device remain unchanged with bending radii down to 0.7 mm, which represents a significant improvement in mechanical flexibility over previously demonstrated semiconductor NM photodetectors (37).

## Summary

In this article, we provide an overview on flexible integrated photonics. We illustrate through the examples of glass-based bendable and stretchable photonics that clever mechanical designs can lift constraints imposed on intrinsic mechanical properties of constituent materials in flexible systems, thereby allowing the creation of highly compliant device modules out of brittle materials including glass. Inorganic glasses, now formally introduced into the expanded material repertoire for flexible photonics, offer important performance edge compared to organic polymers, including significantly widened accessible range of optical properties, superior thermal and chemical stability, as well as highly versatile processing routes compatible with a diverse set of materials commonly used in photonic integration. We foresee that these useful attributes of glass materials for photonic integration, evidenced by our initial demonstration of flexible glass waveguide-integrated photodetectors, will ultimately pave the path towards a fully integrated flexible photonic circuitry.

## Acknowledgments

Funding support for this work is provided by the National Science Foundation under awards 1453218 and 1506605, and the Department of Energy under grant DE-NA0002509. This work was performed in part at the Harvard University Center for Nanoscale Systems, a member of the National Nanotechnology Infrastructure Network (NNIN) supported by the National Science Foundation under award 0335765.

## References

1. S. E. Miller, *At&T Tech J*, **48**, 2059 (1969).
2. W. S. Wong and A. Salleo, *Flexible electronics: materials and applications*, Springer Science & Business Media (2009).
3. Flexible Electronics Market By Component (Display, Battery, Sensors, and Memory) For Automotive, Consumer Electronics, Healthcare and Industrial Application: Global Industry Perspective, Comprehensive Analysis, Size, Share, Growth, Segment, Trends and Forecast, 2015 – 2021, in, Zion Market Research (2016).
4. D.-H. Kim, N. Lu, R. Ma, Y.-S. Kim, R.-H. Kim, S. Wang, J. Wu, S. M. Won, H. Tao and A. Islam, *Science*, **333**, 838 (2011).
5. S. Takeuchi, T. Suzuki, K. Mabuchi and H. Fujita, *J Micromech Microeng*, **14**, 104 (2003).
6. S. Aikio, J. Hiltunen, J. Hiitola-Keinänen, M. Hiltunen, V. Kontturi, S. Siitonen, J. Puustinen and P. Karioja, *Opt Express*, **24**, 2527 (2016).
7. S. Aikio, M. Zeilinger, J. Hiltunen, L. Hakalahti, J. Hiitola-Keinänen, M. Hiltunen, V. Kontturi, S. Siitonen, J. Puustinen and P. Lieberzeit, *RSC Advances*, **6**, 50414 (2016).
8. B. W. Swatowski, C. M. Amb, S. K. Breed, D. J. Deshazer, W. K. Weidner, R. F. Dangel, N. Meier and B. J. Offrein, in *SPIE OPTO*, p. 862205 (2013).
9. C. Choi, L. Lin, Y. Liu, J. Choi, L. Wang, D. Haas, J. Magera and R. T. Chen, *J Lightwave Technol*, **22**, 2168 (2004).
10. E. Bosman, G. Van Steenberge, B. Van Hoe, J. Missinne, J. Vanfleteren and P. Van Daele, *Ieee Photonic Tech L*, **22**, 287 (2010).
11. T.-J. Peters and M. Tichem, in *SPIE OPTO*, p. 97600D (2016).

12. L. Li, Y. Zou, H. T. Lin, J. J. Hu, X. C. Sun, N. N. Feng, S. Danto, K. Richardson, T. Gu and M. Haney, *J Lightwave Technol*, **31**, 4080 (2013).
13. S. M. Kamali, A. Arbabi, E. Arbabi, Y. Horie and A. Faraon, *Nat Commun*, **7** (2016).
14. H. C. Ko, M. P. Stoykovich, J. Song, V. Malyarchuk, W. M. Choi, C.-J. Yu, J. B. Geddes Iii, J. Xiao, S. Wang and Y. Huang, *Nature*, **454**, 748 (2008).
15. L. Zhu, J. Kapraun, J. Ferrara and C. J. Chang-Hasnain, *Optica*, **2**, 255 (2015).
16. Y. Chen, H. Li and M. Li, *Sci Rep-Uk*, **2**, 622 (2012).
17. C. L. Yu, H. Kim, N. de Leon, I. W. Frank, J. T. Robinson, M. McCutcheon, M. Liu, M. D. Lukin, M. Loncar and H. Park, *Nano Lett*, **13**, 248 (2012).
18. Y. Zou, L. Moreel, H. T. Lin, J. Zhou, L. Li, S. Danto, J. D. Musgraves, E. Koontz, K. Richardson, K. D. Dobson, R. Birkmire and J. J. Hu, *Adv Opt Mater*, **2**, 759 (2014).
19. J. P. Bristow, Y. Liu, T. Marta, S. Bounnak, K. Johnson, Y.-S. Liu and H. S. Cole, in *Photonics West'95*, p. 61 (1995).
20. M. Hikita, R. Yoshimura, M. Usui, S. Tomaru and S. Imamura, *Thin Solid Films*, **331**, 303 (1998).
21. T. Matsuura, J. Kobayashi, S. Ando, T. Maruno, S. Sasaki and F. Yamamoto, *Appl Optics*, **38**, 966 (1999).
22. G. T. Paloczi, Y. Huang and A. Yariv, *Electron Lett*, **39**, 1650 (2003).
23. H. Ma, A. Y. Jen and L. R. Dalton, *Adv Mater*, **14**, 1339 (2002).
24. L. Li, P. Zhang, W.-M. Wang, H. Lin, A. B. Zerdoum, S. J. Geiger, Y. Liu, N. Xiao, Y. Zou and O. Ogbuu, *Sci Rep-Uk*, **5**, 13832 (2015).
25. L. Fan, L. T. Varghese, Y. Xuan, J. Wang, B. Niu and M. Qi, *Opt Express*, **20**, 20564 (2012).
26. Y. Zou, D. Zhang, H. Lin, L. Li, L. Moreel, J. Zhou, Q. Du, O. Ogbuu, S. Danto and J. D. Musgraves, *Adv Opt Mater*, **2**, 478 (2014).
27. L. Li, H. Lin, S. Qiao, Y. Zou, S. Danto, K. Richardson, J. D. Musgraves, N. Lu and J. Hu, *Nat Photonics*, **8**, 643 (2014).
28. L. Li, H. T. Lin, S. Geiger, A. Zerdoum, P. Zhang, O. Ogbuu, Q. Y. Du, X. Q. Jia, S. Novak, C. Smith, K. Richardson, J. D. Musgraves and J. J. Hu, *Am Ceram Soc Bull*, **95**, 34 (2016).
29. J. J. Hu, L. Li, H. T. Lin, Y. Zou, Q. Y. Du, C. Smith, S. Novak, K. Richardson and J. D. Musgraves, *Am Ceram Soc Bull*, **94**, 24 (2015).
30. J. Missinne, S. Kalathimekkad, B. Van Hoe, E. Bosman, J. Vanfleteren and G. Van Steenberge, *Opt Express*, **22**, 4168 (2014).
31. Y. Zou, H. Lin, O. Ogbuu, L. Li, S. Danto, S. Novak, J. Novak, J. D. Musgraves, K. Richardson and J. Hu, *Opt Mater Express*, **2**, 1723 (2012).
32. Q. Du, Y. Huang, J. Li, D. Kita, J. Michon, H. Lin, L. Li, S. Novak, K. Richardson and W. Zhang, *Opt Lett*, **41**, 3090 (2016).
33. L. Li, H. Lin, J. Michon, Y. Huang, J. Li, Q. Du, A. Yadav, K. Richardson, T. Gu and J. Hu, *Int J Appl Glass Sci*, **8**, 61 (2017).
34. D.-H. Kim, N. Lu, R. Ghaffari, Y.-S. Kim, S. P. Lee, L. Xu, J. Wu, R.-H. Kim, J. Song and Z. Liu, *Nat Mater*, **10**, 316 (2011).
35. Z. Han, V. Singh, D. Kita, C. Monmeyran, P. Becla, P. Su, J. Li, X. Huang, L. Kimerling and J. Hu, *Appl Phys Lett*, **109**, 071111 (2016).
36. D. Ahn, C.-y. Hong, J. Liu, W. Giziewicz, M. Beals, L. C. Kimerling, J. Michel, J. Chen and F. X. Kärtner, *Opt Express*, **15**, 3916 (2007).

37. W. Yang, H. Yang, G. Qin, Z. Ma, J. Berggren, M. Hammar, R. Soref and W. Zhou, *Appl Phys Lett*, **96**, 121107 (2010).